Behavior of the Lorenz-Mie Poles in the Complex Space of Sphere Parameters

Andrey V. Romanov[1, 2, a)] and Maxim A. Yurkin[1, 2]

[1]*Voevodsky Institute of Chemical Kinetics and Combustion, SB RAS, Institutskaya 3, 630090 Novosibirsk, Russia*
[2]*Novosibirsk State University, Pirogova 2, 630090 Novosibirsk, Russia*

[a)]Corresponding author: *a.v.romanov94@gmail.com*

Abstract. We studied the position and motion of poles of Lorenz-Mie (LM) coefficients, responsible for LM resonances, in the space of complex parameters: the size, the refractive index of the sphere, and the refractive index of the host medium. We performed a comprehensive theoretical analysis and classified all resonances according to their asymptotic behavior and origin. In particular, we proved a few lemmas concerning the logarithmic derivatives of Riccati-Bessel functions and used them to prove the absence of LM poles in some areas of the complex plane (depending on the host medium). We also performed extensive numerical calculations of pole trajectories, which fully confirm all theoretical predictions and provide additional details in the intermediate range of size parameters.

INTRODUCTION

LM resonances, also known as morphology-dependent resonances (MDRs), manifest themselves in sharp peaks of the scattering quantities of a homogeneous sphere under variation of any problem parameters. They have been known as long as the LM theory itself, and their intensive exploration started about 50 years ago with the appearance of computers. The fundamental results of this exploration are mostly covered by an extensive review [1], while practical applications continue to appear from characterization [2], switching and sensing [3], to the development of nanomaterials [4]. However, the richness of LM resonances is far from being exhausted, especially with respect to arbitrary complex values of refractive indices of the host medium and the sphere, which are related to complex values of permittivities ε_1 and ε_2, respectively. The latter lead to arbitrary complex values of relative refractive index $m \stackrel{\text{def}}{=} \sqrt{\varepsilon_2/\varepsilon_1}$, size parameter $x \stackrel{\text{def}}{=} k_1 r$, where r is a sphere radius and $k_1 \stackrel{\text{def}}{=} \omega\sqrt{\varepsilon_1\mu_0}$ is wavenumber in the host medium, μ_0 is the vacuum permeability, and $y \stackrel{\text{def}}{=} mx$. The case of absorbing host media has been recently gaining renewed interest [5,6]. Further we consider time-harmonic problem with the implicit $\exp(-\mathrm{i}\omega t)$ convention.

LM resonances are naturally related to the complex poles of LM coefficients. In the following we describe a comprehensive analysis of all these poles as trajectories in 2D complex space $\mathbb{C}^2$, either (x, y) or (x, m), being limited only by assumption of non-magnetic materials. First, we analyze the LM poles in complex plane of x for fixed y and vice versa, considering both asymptotic cases (large and small $|x|$ and/or $|y|$) and intermediate ones. This leads to rigorous description of the pole-free region in $\mathbb{C}^2$. We also describe the motion of the poles under variation of the second parameter, leading to classification of the poles according to their behavior and origin. Next, we translate the above analysis to the space (x, m) that is more relevant for practical applications. Finally, we present the results of extensive numerical calculations of pole trajectories, which fully confirm all theoretical predictions.

MAIN ANALYTICAL RESULTS

LM coefficients for the external field are given by [7] (at least for a passive host medium)

5th International Conference on Metamaterials and Nanophotonics METANANO 2020
AIP Conf. Proc. 2300, 020104-1–020104-4; https://doi.org/10.1063/5.0032044
Published by AIP Publishing. 978-0-7354-4034-0/$30.00

$$a_n \stackrel{\text{def}}{=} \frac{m\psi_n(mx)\psi_n'(x) - \psi_n(x)\psi_n'(mx)}{m\psi_n(mx)\xi_n'(x) - \xi_n(x)\psi_n'(mx)}, \qquad b_n \stackrel{\text{def}}{=} \frac{\psi_n(mx)\psi_n'(x) - m\psi_n(x)\psi_n'(mx)}{\psi_n(mx)\xi_n'(x) - m\xi_n(x)\psi_n'(mx)}, \tag{1}$$

where $n \in \mathbb{N}$ and ψ_n, ξ_n are the Riccati–Bessel functions: $\psi_n(z) \stackrel{\text{def}}{=} \sqrt{\pi z/2}\, J_{n+1/2}(z)$, $\xi_n(z) \stackrel{\text{def}}{=} \sqrt{\pi z/2}\, H^{(1)}_{n+1/2}(z)$. The poles of coefficients (1) take place when the corresponding denominators vanish:

$$a_n\colon \quad m\psi_n(mx)\xi_n'(x) - \xi_n(x)\psi_n'(mx) = 0, \qquad b_n\colon \quad \psi_n(mx)\xi_n'(x) - m\xi_n(x)\psi_n'(mx) = 0. \tag{2}$$

Thus, the problem is reduced to describing the roots of these equations under the variation of variables x and m in the complex plane. We can also rewrite is in terms of x and y:

$$a_n\colon \quad \frac{f_n(x)}{x} = \frac{g_n(y)}{y}, \qquad b_n\colon \quad x f_n(x) = y g_n(y). \tag{3}$$

where $f_n(z) \stackrel{\text{def}}{=} \xi_n'(z)/\xi_n(z)$ and $g_n(z) \stackrel{\text{def}}{=} \psi_n'(z)/\psi_n(z)$ are logarithmic derivatives. We proved two lemma concerning the properties of these functions not found in the literature, here we show only the most interesting results:

$$\begin{gathered} 0 \le \arg z \le \pi \Rightarrow \arg f_n(z) \text{ is between } \pi/2 \text{ and } \pi - \arg z, \\ 0 < |\arg z| < \pi \Rightarrow \arg g_n(z) \text{ is between } -\arg z \text{ and } \arg \bar{z}, \end{gathered} \tag{4}$$

where $\bar{z}$ is the complex conjugate of z. Other properties include the asymptotic behavior for $|z| \gg n$ and $|z| \ll n$.

Physically, $\arg x, \arg y \in (-\pi/2, \pi/2]$ based on the standard branch-cut definition of the complex square root. Then Eqs. (3), (4) imply that for $\arg x \in [0, \pi/2)$ the resonant values of y must satisfy

$$a_n\colon \quad \arg y \in \left(\arg x - \frac{\pi}{2}, 0\right), \qquad b_n\colon \quad \arg y \in \left(\frac{\arg x}{2} - \frac{\pi}{4}, 0\right). \tag{5}$$

Thus, all LM resonances with fixed x (ε_1) satisfy one of the following equivalent conditions:

$$\arg y \in \left(\arg x - \frac{\pi}{2}, 0\right) \Leftrightarrow \arg m \in \left(-\frac{\pi}{2}, -\arg x\right) \Leftrightarrow \arg \varepsilon_2 \in (\arg \varepsilon_1 - \pi, 0). \tag{6}$$

The obtained condition on ε_2 is exactly the one conjectured in [8] for particles of arbitrary shape. That conjecture additionally includes the line $\arg \varepsilon_2 = \arg \varepsilon_1 - \pi$, corresponding to the essential spectrum of the scattering integral operator. The latter is different from the discrete spectrum, corresponding to the MDRs discussed in this paper. For $\arg x \to \pi/2 - 0$ Eq. (5) implies $\arg y \to -0$, denoting that both limits are approached strictly from the left.

Using the asymptotes of f_n and g_n, we can characterize the solutions of Eqs. (3) more precisely, especially with respect to $|y|$ and $|x|$. We identified 4 main areas for these functions: the asymptotic limits for $|z| \gg n$ and $|z| \ll n$, intermediate region $|z| \sim n$ (all should be far from the zeros and poles of $f_n(z)$ and $g_n(z)$) and *special region*, which contains the zeros and poles of f_n and g_n. In case of g_n the special region is located on the positive real axis, since it corresponds to the known zeros of $\psi_n(z)$ and $\psi_n'(z)$, i.e. of Bessel functions. In case of f_n, the special region almost coincides with the intermediate region in the lower complex half-plane, since $\xi_n(z)$ and $\xi_n'(z)$ has zeros uniformly distributed along the eye-shaped curve in that area (as zeros of Hankel functions).

Solving Eqs.(3) for fixed x, $g_n(y)$ can achieve any complex value for y between zeros and poles of this function. Consequently, the resonant values of y will be located in the special region and asymptotically will tend to the zeros of the Bessel function $\psi_n(y)$ or its derivative $\psi_n'(y)$ with variation of x between zero and infinity. We denote these roots as Bessel-zero resonances (BZRs) – in the following we will see that they correspond to the typical narrow MDRs for dielectric or low-absorbing spheres. Similarly, for fixed y, x-roots of Eqs.(3) located in the special region of $f_n(x)$ are denoted as Hankel-zero resonances (HZRs).

Substituting the asymptotes of f_n and g_n into Eqs. (3) we found solutions only for two combinations of $|x|$, $|y|$:

$$\begin{gathered} a_n, b_n\colon\ |x|, |y| \gg n \Rightarrow x = y, \arg y \in [-\pi/2, 0), \\ a_n\colon\ |x|, |y| \ll n \Rightarrow y = -\mathrm{i}\,\mathrm{sgn}(\arg x) x \sqrt{\frac{n+1}{n}}, \end{gathered} \tag{7}$$

Analyzing the previous results in coordinates of x and m we obtained:

$$a_n, b_n\colon\ m \to 1 \ \Rightarrow\ |x| \to \infty, \qquad \arg x \in [-\pi/2, 0), \tag{8}$$

$$a_n\colon\ m \to \pm \mathrm{i}\sqrt{\frac{n+1}{n}} \ \Rightarrow\ |x| \to 0, \operatorname{sgn}(\arg x) = \mp 1. \tag{9}$$

Furthermore, Eqs. (3) has no solutions for $m = 1$. Therefore all x-roots move to ∞ when $m \to 1$.

NUMERICAL CALCULATIONS AND DISCUSSIONS

We performed extensive numerical simulations of the positions of the roots of Eqs. (3), applying the Newton–Raphson method, and obtained 3-dimensional trajectories of resonances for specific modulus (or argument) of a fixed variable. Continuity of the functions implies continuity of the root trajectories.

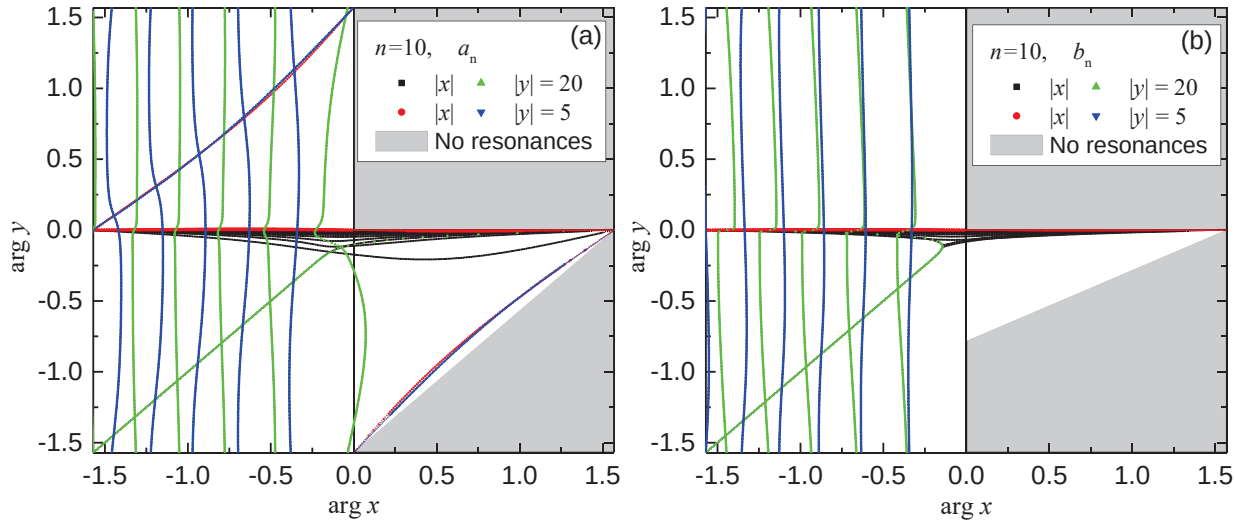

FIGURE 1. Location of LM resonances for a_{10}(a) and b_{10}(b) coefficients in coordinates $\arg x$, $\arg y$ calculated for fixed $|x|$ (black and red dots), and fixed $|y|$ (green and blue dots), the gray area is proven to be resonance-free.

As a single example, we present the resonances positions in coordinates $\arg x$, $\arg y$ in Fig. 1. It shows how exactly resonances fill the regions, which are not amenable to rigorous mathematical analysis. We can observe all different types of resonances: $x \approx y$ resonances in the 3rd quadrant for large sizes (both for a_n and b_n), $x \approx y\sqrt{\pm \mathrm{i}(n+1)/n}$ resonances for small size (only for a_n), BZRs located near $\arg y = 0$, and HZRs (close-to-vertical green and blue lines on negative $\arg x$ axis). The appearance of asymptotic types at such moderate scales ($|z| \sim 2n$ or $n/2$) is due to the exponential behavior of the Bessel and Hankel functions, as explained in [9].

The first manifestations of the resonance structure were noticed in the host scattering cross-sections for non-absorbing media [1,7], which corresponds to real x. Therefore, the closer the x-poles (for fixed m) approach the real axis – the brighter the resonance structure appears. Figure 1 shows that for real (or slightly absorbing) m only BZRs are at a sufficiently small distance to be observable. The HZRs were directly observed only in one case – the case of negative dielectric permittivity, the so-called surface modes or plasmon resonances [10,11]. Their manifestation is associated with an asymptotic resonance for imaginary m (Eq. (9)) in which case one of the HZR approaches the real axis when m gets close to $\pm \mathrm{i}\sqrt{(n+1)/n}$.

CONCLUSION

We analyzed the locations of the LM resonances in complex planes of x, y, and m. Based on the newly proven properties of $f_n(z)$ and $g_n(z)$ we identified the areas of complex space of parameters where resonances cannot appear. In coordinates x, y they are described as $\arg x \geq 0$ and ($\arg y \geq 0$ or $\arg y \leq \arg x - \pi/2$), in agreement with previous theoretical hypothesis for particles of arbitrary shape. We also qualitatively described the behavior of resonance equations in various regions of the complex plane, which allowed us to classify all observed resonances into the BZR, HZR, and asymptotic ones. BZRs are located near the real axis of y and is commonly observed in

applications. HZRs are located along the eye-shaped curve in the lower complex half-plane of x around the origin. Two types of asymptotic resonances related to m approaching special values correspond to either one resonance moving to zero x (plasmon type) or all resonances – to infinity (the case of negligible scattering).

The results were confirmed by simulation with the Newton method for root searching. Additionally, we demonstrated the behavior of resonances in various cases using 2D trajectories, by fixing one parameter and varying the other. Those extensive simulations will be discussed in details at the conference. Some of our results reproduce those found in the literature, but some provide new insights that potentially can lead to interesting experimental applications.

ACKNOWLEDGMENTS

We thank James A. Lock and Vadim A. Markel for insightful discussions. The research has been supported by the Russian Science Foundation (project number 18-12-00052).

REFERENCES

1. S.S. Hill and R.E. Benner, "Morphology-dependent resonances," in *Optical Effects Associated with Small Particles*, edited by R.K. Chang and P.W. Barber (World Scientific, Singapore, 1988), pp. 1–61.
2. G. Chen, M. Mazumder, R.K. Chang, C. Swindalt, and W.P. Ackert, Prog. Energy Combust. Sci. **22**, 163–188 (1996).
3. M.F. Limonov, M.V. Rybin, A.N. Poddubny, and Y.S. Kivshar, Nat. Photon. **11**, 543–554 (2017).
4. Q. Zhao, J. Zhou, F. Zhang, and D. Lippens, Materials Today **12**, 60–69 (2009).
5. M.I. Mishchenko and P. Yang, J. Quant. Spectrosc. Radiat. Transfer **205**, 241–252 (2018).
6. M.I. Mishchenko, J.M. Dlugach, J.A. Lock, and M.A. Yurkin, J. Quant. Spectrosc. Radiat. Transfer **217**, 274–277 (2018).
7. C. Bohren and D. Huffman, *Absorption and Scattering of Light by Small Particles* (Wiley, New York, 1983).
8. M.A. Yurkin and M.I. Mishchenko, Phys. Rev. A **97**, 043824 (2018).
9. M.I. Tribelsky and A.E. Miroshnichenko, Phys. Rev. A **93**, 053837 (2016).
10. B.S. Luk'yanchuk, M.I. Tribelsky, V. Ternovsky, Z.B. Wang, M.H. Hong, L.P. Shi, and T.C. Chong, J. Opt. A **9**, S294 (2007).
11. M.I. Mishchenko and J.M. Dlugach, OSA Continuum **2**, 3415 (2019).